Title

PERFORMANCE OF A VALDRE HEATING AND TILTING STAGE IN THE SIEMENS ELECTRON MICROSCOPE

Author

Sturcken, E.F.

Publication Date

1968-04-01

University of California

Ernest O. Lawrence Radiation Laboratory

PERFORMANCE OF A VALDRÉ HEATING AND TILTING STAGE IN THE SIEMENS ELECTRON MICROSCOPE

E. F. Sturcken

April 1968

DISCLAIMER

UCRL-17773

UC-37 Instruments
TID-4500 (51st Ed.)

UNIVERSITY OF CALIFORNIA
Lawrence Radiation Laboratory
Berkeley, California

AEC Contract No. W-7405-eng-48

PERFORMANCE OF A VALDRÉ HEATING AND TILTING STAGE IN THE SIEMENS ELECTRON MICROSCOPE

E. F. Sturcken

April 1968

PERFORMANCE OF A VALDRÉ HEATING AND TILTING STAGE IN THE SIEMENS ELECTRON MICROSCOPE

E. F. Sturcken

Inorganic Materials Research Division, Lawrence Radiation Laboratory, University of California, Berkeley, California*

I. SUMMARY AND CONCLUSIONS

A Valdré type heating and tilting stage was constructed for the Siemens electron microscope. The design characteristics and performance of the stage are described.

The stage was found to have rapid temperature response, smooth tilting capability and negligible drift of the area under observation at temperatures up to 1000°C.

The performance of the hot stage was tested by employing it to observe the HCP to FCC transformation (417°C) of cold rolled cobalt and the temperature dependence of Bloch type magnetic domain walls in HCP cobalt. With the specimen at 450°C the transformation was complete in a few minutes. The HCP grains nucleated heterogeneously and, in seconds, grew to a grain size of about 0.5μ. The transformation temperature was used to calibrate the specimen thermocouple. Domain walls along [0001] were observed to widen and became diffuse at 150°C and disappeared below 300°C as predicted from previous measurements of magnetization versus temperature versus crystallographic direction. These measurements have shown that the magnetocrystalline energy favors easy magnetization along [0001] from 0 to 250°C and easy magnetization along $\langle 11\bar{2}0\rangle$ and $\langle 10\bar{1}0\rangle$ above 250°C.

* Now at the Savannah River Laboratory, E. I. du Pont de Nemours and Co., Aiken, South Carolina.

An important limitation of high temperature microscopy appears to be the physical instability of foils in the < 2000Å thickness range. Even though devices and techniques can be developed to prevent bending and contamination, the high surface to volume ratio of the foils makes them inherently unstable. Cobalt has a low vapor pressure (< 10^{-10} atm) and high melting point (1495°C); however foils of cobalt contracted, thickened and formed numerous holes at 700°C.

Procedures for installing the heating and tilting stage in the microscope are described in an appendix.

II. INTRODUCTION

The heating and tilting stage to be described was constructed at Berkeley from design data provided by Prof. U. Valdré, Instituto di Fisica, University of Bologna, Italy. The design philosophy and design details have been discussed in several papers by Valdré.[1-3] The present report gives only a brief summary of design characteristics, then emphasizes the solutions to several problems that were encountered during the construction and operation of the stage.

The phase transformation and magnetic domain studies are of a preliminary nature and intended primarily to test the performance of the heating and tilting stage. The micrographs are not of the best quality because the objective pole piece was a "home-made" one and was not polished, heat treated and oriented to give maximum resolution. It would have also been desirable to use an anti-contamination device.

III. DISCUSSION

A. Design Characteristics

The heating and double-tilting specimen holder, Figs. 1 and 2, is designed to have a minimum loss in resolution, to tilt at least 20 degrees in any direction, to be inserted in the standard object stage through the standard air lock and to cover a specimen area of 0.8 square millimeter.

The specimen is heated by clamping it to a platinum disc indirectly heated by a spiralled tungsten filament. With this method the specimen temperature is uniform and independent of the specimen. No special size or shape of sample is necessary so the method is ideal for foils prepared by window electropolishing techniques.[4]

The furnace section of the specimen holder is materially and mechanically designed so that it has low heat capacity and reaches relatively high temperatures for a power input of only a few watts. The low heat capacity and power input give the heating system fast response and avoid possible damage to the microscope.

The standard object stage is modified, Fig. 3, to provide spring loaded push pins for heating and thermocouple contacts and push pins and gears for tilting and rotating the specimen. The push pins and gears of the object stage are driven by a triple drive system, Fig. 4, which has two entrance ports for power and thermocouple leads and other devices. The drive system is screwed into the front stereo hole of the objective section of the microscope. A standard cold finger may be used as an anticontamination device in the spare stereo hole on the right side of the objective section.

Both the stage and the drive system are "universal" in that they can be used with three different types of Valdré specimen holders; the heating and double-tilting holder,[2] the cooling and double-tilting holder[3] and the rotating double-tilting holder.[3] Only the former is described in the present report.

To accomodate the new specimen holder the specimen level is raised 2 millimeters in the holder and the bore of the top portion of the objective pole piece is increased from 6.5 to 9.0 millimeters. Valdré has shown[2] the resulting pole piece to have a resolution of 15Å.

The magnification of the heating and tilting stage was determined with a diffraction replica grating and found to be reduced from that of the standard Siemens double tilting stage by a factor of 1.3 to 1.4 (see Appendix 2).

B. The Thermocouple

The thermocouple was made of 0.005 inch wires of platinum and platinum plus 10% rhodium alloy. The junction was kept small by employing a hydrogen-oxygen torch with a hypodermic needle tip. A large junction will act as a "heat sink" near the specimen.

To minimize the amount of bending during tilting, the thermocouple wires enter the ball near one of the pivot points, Figs. 1 and 2, on the gimbal ring. The thermocouple junction is in direct contact with the platinum disk, Fig. 1, on which the sample is clamped. The junction is press fitted and cemented (to keep it from moving during tilting) into a hole drilled through the ball, Fig. 1, in which the disk is seated. Because of the small clearance between the ball and the gimbal ring it was necessary to machine a 0.003 inch groove in the ball to prevent the thermocouple wires from jamming between the ball and the gimbal ring and thereby inhibiting the tilting action.

C. The Heating Element

The heating element was fabricated by winding 80 turn/inch of 0.003 inch diameter tungsten wire on a .010" diameter mandrel. The filament is spiralled to reduce the effects of the magnetic field produced by the filament current.

The Al_2O_3 filament coating, obtained from commercial sources, broke off several times during heating and tilting and short-circuited the furnace to the holder. The coating operation is critical because applying thick coatings or "potting the filament" to insure electrical insulation, increases the heat capacity and thereby decreases the temperature response. A ceramic bonding element called Eccoceram CS* has been found resistant to cracking. However, it is only good to a filament temperature of 1000°C and a specimen temperature of about 700°C. Experiments are in progress on a tough ceramic coating that will be good to a filament temperature of 2200°C. The coating must not only be crack and temperature resistant, but it must be applicable in thin coatings. Mounting the filament rigidly would eliminate cracking but would also restrain the tilting action.

The electrical connection to the spiralled tungsten heating element was a 0.010 inch diameter gold wire, Fig. 1, plated with about 0.002 inch of nickel** at the points where it was spot welded to the tungsten. The gold is quite flexible and takes a lot of bending without breaking. Experience suggests that even larger diameter gold wire could be used without inhibiting the tilting action, if it was desired to operate the holder at temperatures higher than 1000°C.

---
* Emerson and Cuming, Inc., Canton, Massachusetts.
** Private correspondence, U. Valdré.

The gold wire leads are soldered to printed gold circuit boards, Figs. 1 and 2, which make contact with the copper push pins of the object stage when the holder is inserted in the stage.

D. Pt-Pt-10% Rh Components

To avoid magnetic effects and corrosion, the central portion of the specimen holder was constructed of a platinum plus 10% rhodium alloy, Fig. 1. However, the elimination of these problems introduced another one; namely, galling between the ball and tubular lever, at the pivot points of the gimbal ring and ball, and at points where the pushers and counter-pushers contact the lever, Fig. 2. The galling caused abrupt and rough tilting action.

The problem was eliminated by burnishing all of these parts with a solid molybdenum lubricant. It may also be possible to use more rhodium in the platinum rhodium alloy. However, if the alloy is made too hard it is difficult to machine. To ensure dimensional control the alloy was machined close to final dimensions then annealed and machined to final dimensions.

E. Miscellaneous

The rotation functions of the object stage and triple drive are not used for the heating and double-tilting specimen holder, hence this drive system was removed and stored and an "O" ring sealed plug, Fig. 9b, inserted in its place.

Because of the delicate nature of the specimen holder it is easy to bend the heater and thermocouple leads and cause them to short circuit when screwing the holder into the threaded suspension in the specimen air lock. Hence some sort of tool should be fabricated to grip the specimen holder when performing this operation.

IV. RESULTS

A. Time-Temperature Response Measurements

The time temperature response of the stage was continuously recorded with a millivolt recorder. Time versus temperature plots for two heating and cooling cycles are shown in Fig. 5. The specimen heats from room temperature to 825°C in about one minute and cools from 825° to 200°C in about six minutes. The power input for 825°C was only 4.5 watts.

B. HCP to FCC Transformation in Cobalt

The foils were prepared by cold rolling 0.005 inch cobalt strips to a thickness of 0.001 inch then thinning electrolytically by the window method.[4] Cobalt deforms predominantly by basal slip[5] hence the plane of the foil had a strong [0001] texture.

The transmission electron microstructures and selected area diffraction patterns are shown, Fig. 6, for the foil at room temperature and above the transformation temperature (450°C). The room temperature SAD pattern shows the HCP crystal structure. The 450°C SAD pattern shows a number of FCC grains and some ring structure due either to small FCC grains or residual HCP as-rolled grains. Random indexing of the spots in the 450°C SAD pattern showed that a number of grains have their (111) plane in the plane of the foil as might be expected since they are predominantly nucleated from HCP grains with (0001) parallel to the plane of the foil.

The initial rate of grain growth is very rapid. The order of magnitude change in grain size, Fig. 6, between the as-rolled and transformed cobalt took place in a few minutes.

C. Temperature Sensitivity of Magnetic Domains in Cobalt

The cobalt foils were prepared from .005 inch cobalt sheet, of 99.99% purity, cold rolled to .002 inch, then heat treated in vacuum 3 hours at 900°C. Magnetic domain walls of the Bloch type are shown by the out-of-focus[6] method in Fig. 7. For a study of the application of the out-of-focus method to nickel and cobalt, the reader is referred to the work of Silcox.[7] In Fig. 7a the domains are at room temperature. As the temperature is increased to 150°C, Fig. 7c, the domain walls widen and become diffuse and are difficult to show by the out-of-focus method. Finally at a temperature of 300°C, Fig. 7d, the domains have disappeared completely. The thickening and disappearance of the domains may be explained by reference to the theory of magnetocrystalline energy[8] that is the part of the free energy that directs the magnetization along definite crystallographic direction of "easy magnetization."

For hexagonal cobalt the magnetocrystalline energy, E_c, is given by Stoner[9] as

$$E_c = K_1 \sin^2\theta + K_2 \sin^4\theta \qquad (1)$$

where θ is the angle the magnetization makes with the c-axis and K_1 and K_2 are the anisotropy constants. The equation assumes isotropy in the basal plane. The experimental data of Honda and Masumoto,[10] Fig. 8, and Sucksmith and Thompson[11] on magnetization versus temperature versus field strength for $[10\bar{1}0]$ and $[11\bar{2}0]$ show that basal isotropy is a good assumption. Honda and Masumoto[10] have used the same data to plot the constants K_1 and K_2 as a function of temperature, Fig. 9. Note that, as the temperature is increased, the energy, E_c, available for easy magnetization along [0001] decreases until at 250°C, $K_1 + K_2 = 0$ and the magnetization is isotropic. At higher temperatures, Fig. 8, the magnetization becomes difficult along [0001] and easy along $[11\bar{2}0]$ and $[10\bar{1}0]$.

Let us now offer an explanation for the thickening and disappearance of the domain walls. The foil normal of the diffraction pattern, Fig. 7b, is $[\bar{1}2\bar{1}0]$ and [0001] in the plane of the foil; hence the magnetization is maximum in the plane of observation. Note that, as expected, the trace of the domain wall is along [0001]. The Bloch type domain walls of Fig. 7 are transition layers of many atomic planes over which the spin gradually reverses direction. The magnetocrystalline energy limits the width of this transition layer (domain wall). At room temperature, E_c in Eq. (1) is large so the domain walls are sharp, Fig. 7a. At 150°C, E_c is small and the domain walls are wide and difficult to observe, Fig. 7c. The width of the wall also depends on the foil thickness and the component of magnetization in the plane of the foil; however these factors were held constant in the present experiment. At 300°C, E_c is negative, magnetization is difficult along [0001], Fig. 8, and no domain walls are observable, Fig. 7d.

At these higher temperatures the easy directions of magnetization are the a-axes, hence domain walls should be observable along $\langle 11\bar{2}0 \rangle$ and $\langle 10\bar{1}0 \rangle$, however no experiments were performed in the present work to observe them. There may be complicating factors due to the increased number of "easy" directions ($[10\bar{1}0]$, $[1\bar{1}00]$, $[01\bar{1}0]$, $[11\bar{2}0]$, $[\bar{1}2\bar{1}0]$, $[\bar{2}110]$) of magnetization.

D. Temperature Instability of Thin Foils

During the high temperature tests of the specimen holder it was consistently observed that the cobalt foils developed many holes at temperatures of 700°C and higher. Even at 1060°C the vapor pressure of cobalt is only 1.285×10^{-9} atm, so that high evaporation rates are not expected, nor do the holes appear to be formed by tearing due to restraint or stress of some sort from the supporting grid. An example of holes formed in a cold rolled cobalt foil is shown in Fig. 10. There has also been evidence that gold* and copper** behave similarly at about 500°C.

If one considers a foil section 1 mm^2 by 1500 Å thick, it has a surface to volume ratio 140 times the ratio of a sphere of the same volume. Since the surface energy is quite high, the foil may thicken and form holes, as the temperature is raised, to reduce its surface energy. It is also possible that a very high temperature excursion melted the sample locally and produced the holes. However, in the present study the good agreement of the thermocouple readings with the transformation temperature of cobalt gives reasonable assurance that no temperature excursions are occurring.

If these observations are supported by further experiment, high temperature studies on metals will have to be performed on high energy microscopes where the thickness of foils will be in the micron range.

---

* Private correspondence, M. Yokota, University of California, Berkeley.

** Private correspondence, D. E. Rawl and M. R. Louthan, Savannah River Laboratory, Aiken, South Carolina.

ACKNOWLEDGEMENTS

The author is grateful to Prof. Ugo Valdrè of the University of Bologna, Italy for the design data and helpful correspondence during the course of construction; to J. W. Bryan of LRL for the precision machining and for his ingenuity in solving a number of mechanical problems; to Dr. P. J. C. Gallagher of the Ford Motor Company for passing on his experience and suggestions from the construction of an earlier model Valdré hot stage; to Dr. A. G. Fitzgerald for helpful discussions and to Prof. Gareth Thomas for initiating the project and for encouragement and helpful discussions.

This work was performed under the auspices of the United States Atomic Energy Commission.

REFERENCES

1. U. Valdré, J. Sci. Inst. 39, 278 (1962).
2. U. Valdré, J. Sci. Inst. 42, 853 (1965).
3. U. Valdré, A Universal Specimen State and Combined Cartridges for an Electron Microscope, paper presented at Sixth International Congress for Electron Microscopy, Kyoto, Japan (1966).
4. R. Nicholson, G. Thomas and J. Nutting, J. Brit. J. Appl. Phys. 9, 25 (1958).
5. D. S. Eppelsheimer, and R. C. Wilcox, J. Inst. of Metals, 93, 229 (1964-65).
6. M. E. Hale, H. W. Fuller, and H. Rubinstein, J. Appl. Phys. 30, 789 (1959).
7. J. Silcox, Magnetic Domain Walls in Thin Films of Nickel and Cobalt, Phil. Mag. 8, 7-28 (1963).
8. C. Kittel, Introduction to Solid State Physics, 3rd Edition, (John Wiley and Sons, Inc., New York, 1966), Chapter 15.
9. E. C. Stoner, Rep. Progr. Phys. 13, 83 (1950).
10. K. Honda and H. Masumoto, On the Magnetization of Single Crystals of Cobalt at High Temperatures, Sci. Rep. Tohoku Imperial University 20, 323 (1931).
11. W. Sucksmith and J. E. Thompson, The Magnetic Anisotropy of Cobalt, Proc. Roy. Soc. 225A, 362 (1954).

APPENDIX I

A. Procedure for Installing the Heating and Tilting Stage

The hot stage consists of five sections; the specimen holder, the object stage, the triple drive system, the special objective pole piece, and the instruments for measuring heater current and voltage and thermocouple voltage. The sections will be considered in the order that they are installed in the microscope. It should be emphasized that extreme care must be exercised at all times as the device is very delicate.

1. Triple Drive System

Break the microscope column at the object stage level. Remove the standard object stage and stereo drives. Clean and grease (with silicon) the drive gaskets, the entrance port gaskets and the gasket of the main shaft of the triple drive. Take the four electrical lead wires and the drive wires of the triple drive and hold them together with a piece of electrical "spaghetti". Now, slip the leads and cables through the front stereo hole of the objective section, Figs. 11a and 11b. Remove the spaghetti and screw the lock nut of the triple drive part of the way into the stereo hole. Now, separate the wires and place the "wire positioner", Fig. 11c, on the wires. Make sure that the engagement holes at the end of the cables are vertical, the wire lead port is down, the right drive is turned fully clockwise and the left drive is turned counter-clockwise. The drives are reversed because, as seen in Fig. 3, one of the tilting pins is driven in by rotating a screw clockwise and the other by rotating a screw counter-clockwise.

CAUTION: Do not bend the electrical leads more than necessary to avoid breaking the soldered junction. When the drive is not in the microscope, seat it with the electrical leads up.

2. Object Stage

Check that the keys in the drive engagement holes, Fig. 11c, are vertical so they will engage properly with the drive wires. A tool is provided to rotate the keys. Insert the modified object stage in the normal manner except that the triple drive lock nut must be loosened and the triple drive backed out a short distance to allow the stage to seat properly. Now, carefully push the drive wires into the key holes using the wire positioner (held with tweezers) to center the wires for entry into the holes. The lock nut on the shaft of the triple drive, Fig. 11b, can now be screwed into the stereo hole. Now plug the connecting wires into the connection post, Fig. 11c, and tighten down the screws. Connect the electrical lead wire plug, Fig. 13c, to the plug on the drive system. The heater leads connect to the left post holes, Fig. 11c. The thermocouple leads connect to the right post holes, Fig. 11c. The platinum thermocouple should be connected to the third post hole from the left, Fig. 11c. Use an ohm meter to check that all leads are connected properly and no short or open circuits exist. Close the column.

CAUTION: Do not force the drive wires into the holes. If they do not go in smoothly the keys and holes are not properly aligned.

3. Objective Pole Piece

Loosen the specimen drives, remove all apertures and break the column as shown in Fig. 12. Use the tool provided by Siemens to remove the standard objective pole piece and intermediate pole piece as shown in Fig. 12. Twist the bayonet connection, Fig. 12, to separate the standard objective piece system from the intermediate pole piece system. Now, connect the special objective pole piece, in the same manner, to the intermediate pole piece. Make sure that the fiducial lines on each piece are mated together (rather than 180° apart) when the connection is made. Insert the pole pieces back in the microscope, close the column, insert all apertures and connect the specimen drives. Use a holely carbon film to set the stigmator (see Siemens Instruction Manual) for the special pole piece.

CAUTION: Handle all parts with gloves and place a cover plate over the column while the pole pieces are being exchanged. Remember to set the stigmator back to the original settings when the special pole piece is removed.

4. Specimen Holder

Unscrew the central nut, Fig. 1, of the specimen holder with the tools provided. One tool screws the nut in and the other keeps pressure off the pivot points of the gimbal ring. Mount the specimen, in the normal manner, between two molybdenum grids, drop it in the hole and tighten the nut down. Screw the specimen holder off of the mount and into the threaded suspension of the specimen air lock. The key slot grooved on the body of the holder (not visible in Fig. 1) must be vertical and on the left. If the specimen does not insert into the object stage easily then the key is improperly aligned or the push pins for the heater and thermocouple leads are not receding smoothly. After the specimen is inserted use an ohm meter to read the thermocouple resistance (~1.5Ω) and the heater resistance (~0.9Ω) and to check that the heater leads are not short circuited to the holder or to the thermocouple leads. These measurements are made at the ends of the connecting wires before they are connected to the power supply and thermocouple bridge.

CAUTION: Do not drop the holder, its manufacture required more than 100 hours of precision machining. Do not bend the thermocouple and heater leads on the specimen holder when screwing it into the air lock. Sometimes a "potential" short circuit can be produced that will not show up until the specimen is tilted.

5. Power Supply and Thermocouple Bridge

Connect the heater leads to the power supply. Connect the platinum thermocouple lead wire to the negative post of the thermocouple bridge and the platinum plus 10% Rhodium thermocouple lead wire to the other post. A standard resistance is provided for calibration of the thermocouple bridge.

CAUTION: The furnace resistance is only 0.5Ω, so apply the voltage very slowly with the voltmeter switch set to read amperes. The maximum current required to date was less than 2 amperes.

APPENDIX II

Magnification and camera constant calibration for the heating and tilting specimen holder.

Micrographs (a), (b), (c) and (d) are varying magnifications of a diffraction replica grating at 100 kV using pole piece No. 3 in the Siemens electron microscope. The projector lens current was set to the calibration circle on the image screen. The magnifications read from the magnification meter on the microscope were respectively 4000, 8200, 14,800 and 19,600. The magnification from the calibration gratings are respectively 3110, 6300, 10, 150, and 13,700. Hence the magnification is reduced by a factor of 1.3 to 1.4. These values are approximate since no actual lens currents were measured. The camera constants for the standard double tilting and the heating and tilting specimen holders were determined with an evaporated gold film. The diffraction patterns are shown in micrographs (e) and (f). The camera constants are respectively 2.1 and 2.8. (See micrographs on following page.)

Appendix II

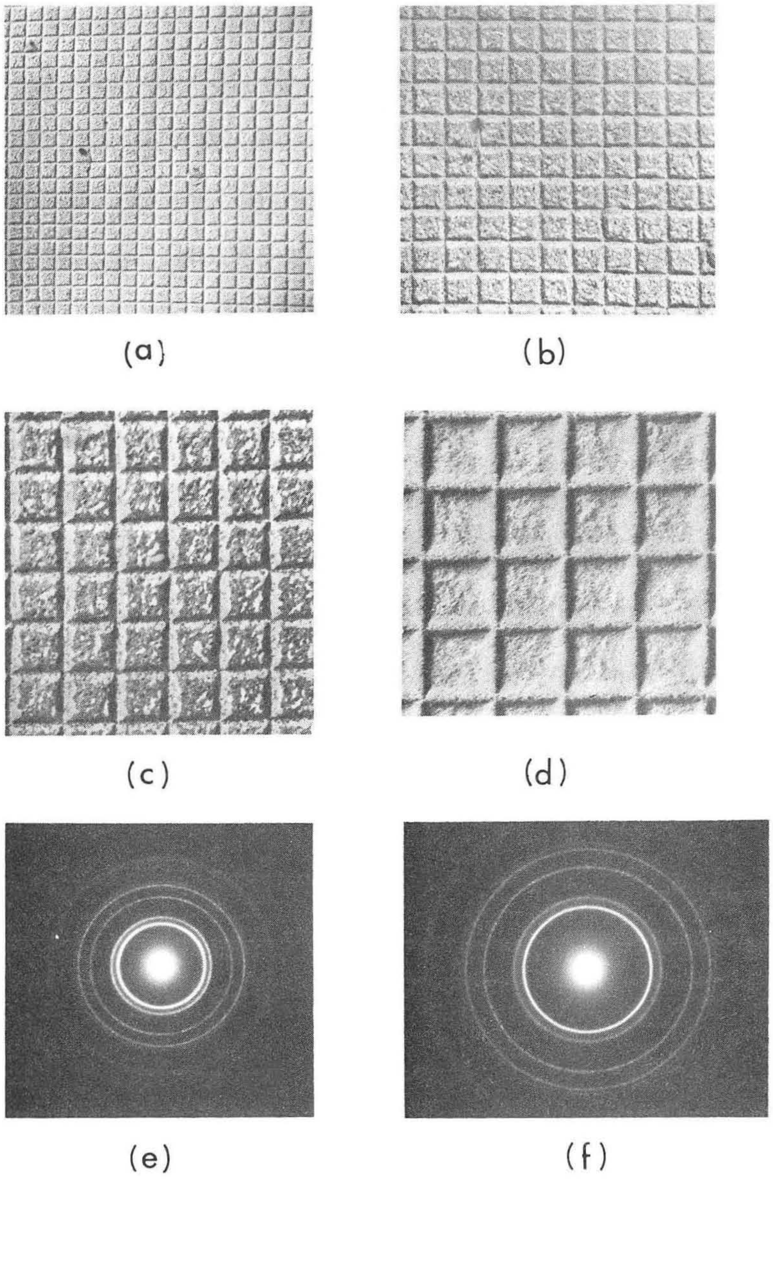

XBB 679-5447

Fig. 1. Specimen holder and components.

1. Siemens size specimen clamping nut and platinum disk clamping nut.
2. Same as one; Hitachi size.
3. Platinum disk.
4. Ball; houses specimen, heater and thermocouple.
5. Gimbal ring and pivot screws.
6. Tilt lever.
7. Ring.
8. Tilt pusher pins.
9. Tilt counter pusher pins and springs.
10. Main body of specimen holder.
11. Gimbal mount.
12. Thermocouple and heater printed (gold) circuit boards.
13. Lever seating ring and screws.
14. Adjustable thread for screwing holder into air lock.
15. Clamping ring for adjustable thread.
16. Gold (0.010" diam.) lead wires to heater.
17. Thermocouple wires (0.005" diam.) Pt-10%Rh.
18. Threaded specimen holder mount.

Parts 1, 2, 4, 6 are Pt-Pt 10%Rh. Part 3 is platinum. Parts 5, 8, 9, 11 are 310 stainless steel (the counter pusher springs are piano wire). The circuit boards are gold-plated fiberglass with a Delrin screw for insulation. The rest of the parts are bronze.

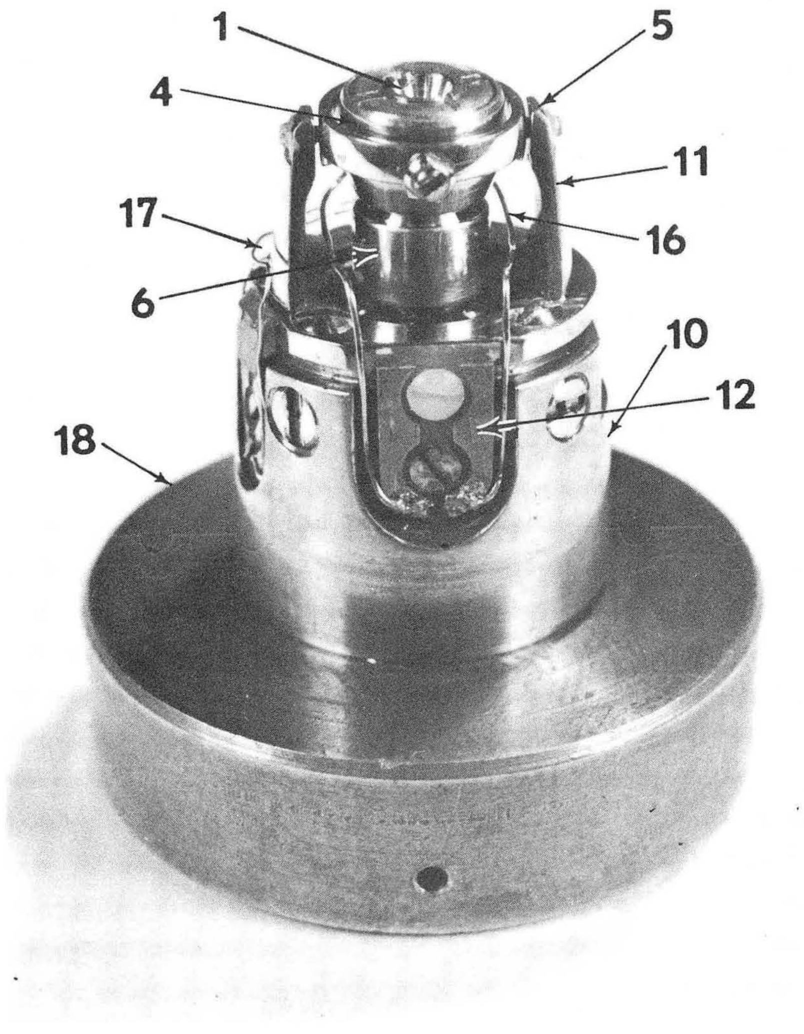

XBB 679-5511

Fig. 1

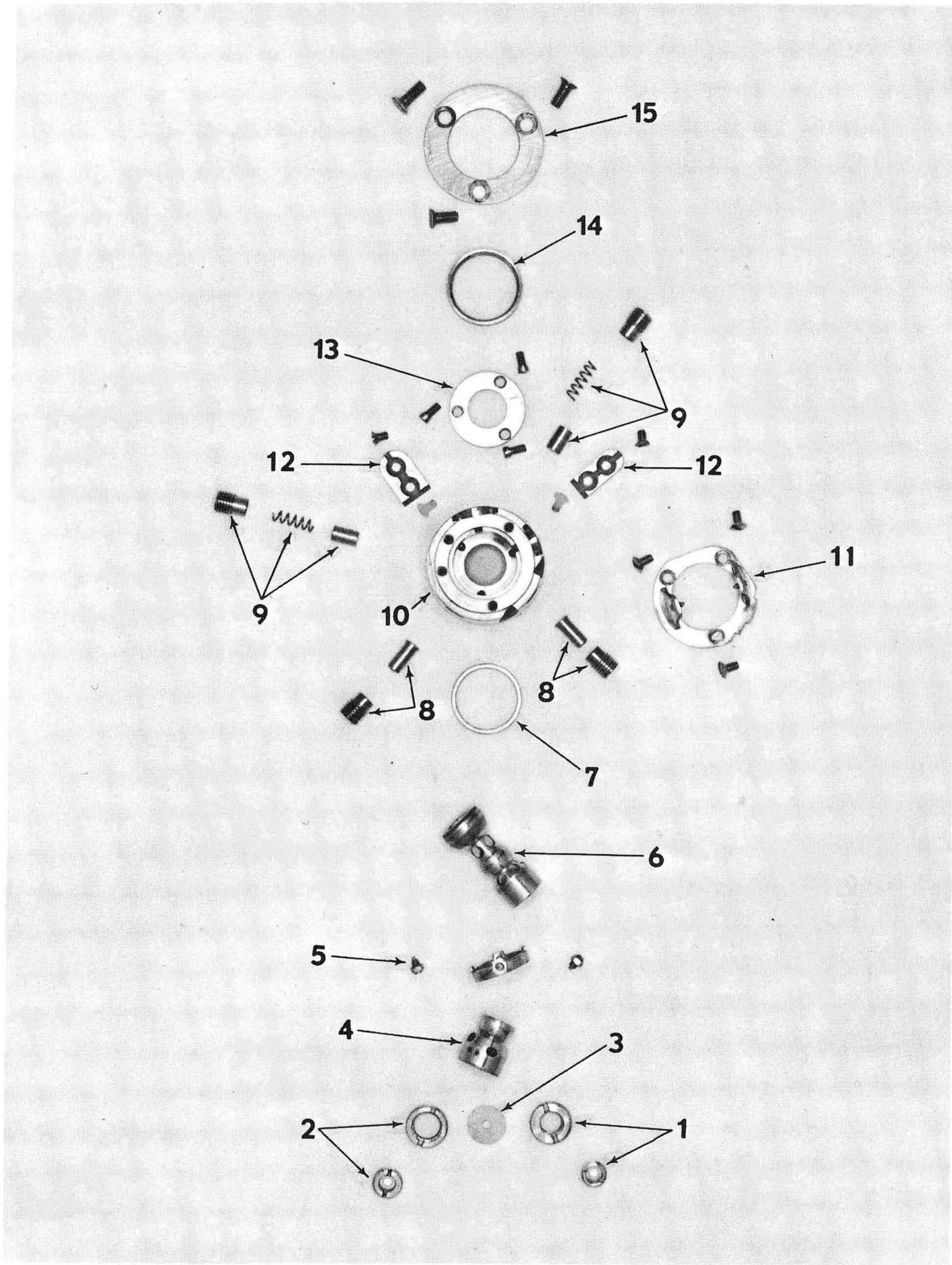

XBB 675-3026

Fig. 1

Fig. 2 Section views of specimen holder.

A is a vertical section, B is a horizontal section at x-x, C is a horizontal section at y-y, D is a side view showing the printed circuit boards, E is an end view. 1) Nut for clamping specimen to platinum disk. 2) Nut for clamping platinum disk against heater. 3) Platinum disk. 4) Pivot pin for suspending gimbal ring. 5) Heater. 6) Ball. 7) Gimbal ring mount. 8) Counter-pusher pin for tilting. 9) Pusher pin for tilting. 10) Main body of specimen holder. 11) Tilting lever. 12) Positioning ring for lever. 13) Threaded ring for screwing specimen holder into air lock. 14) Thermocouple and heater printed circuit boards for electrical contact to object stage. 15) Gold lead wires to heater. 16) Pivot pin for ball.

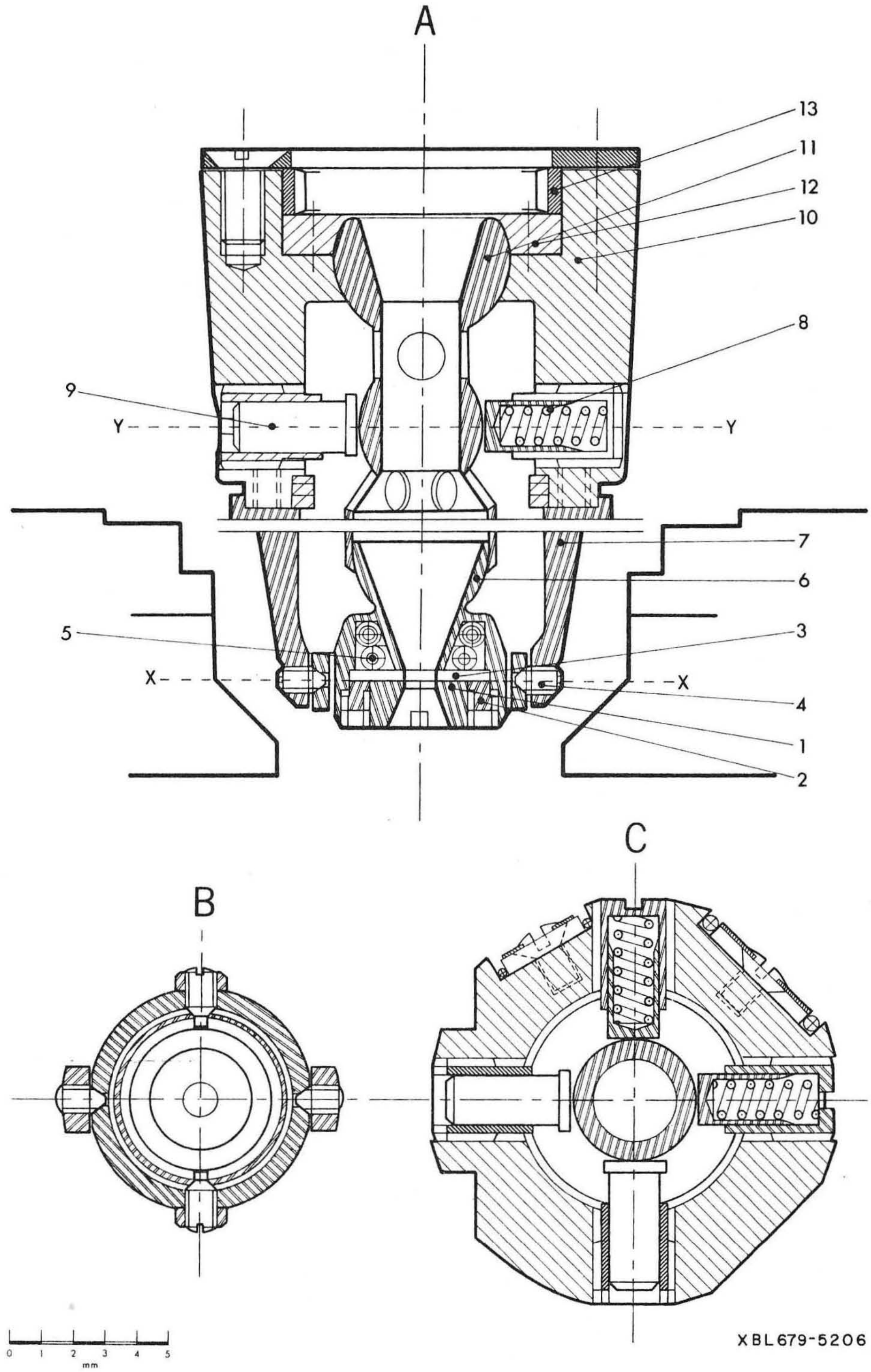

Figure 2

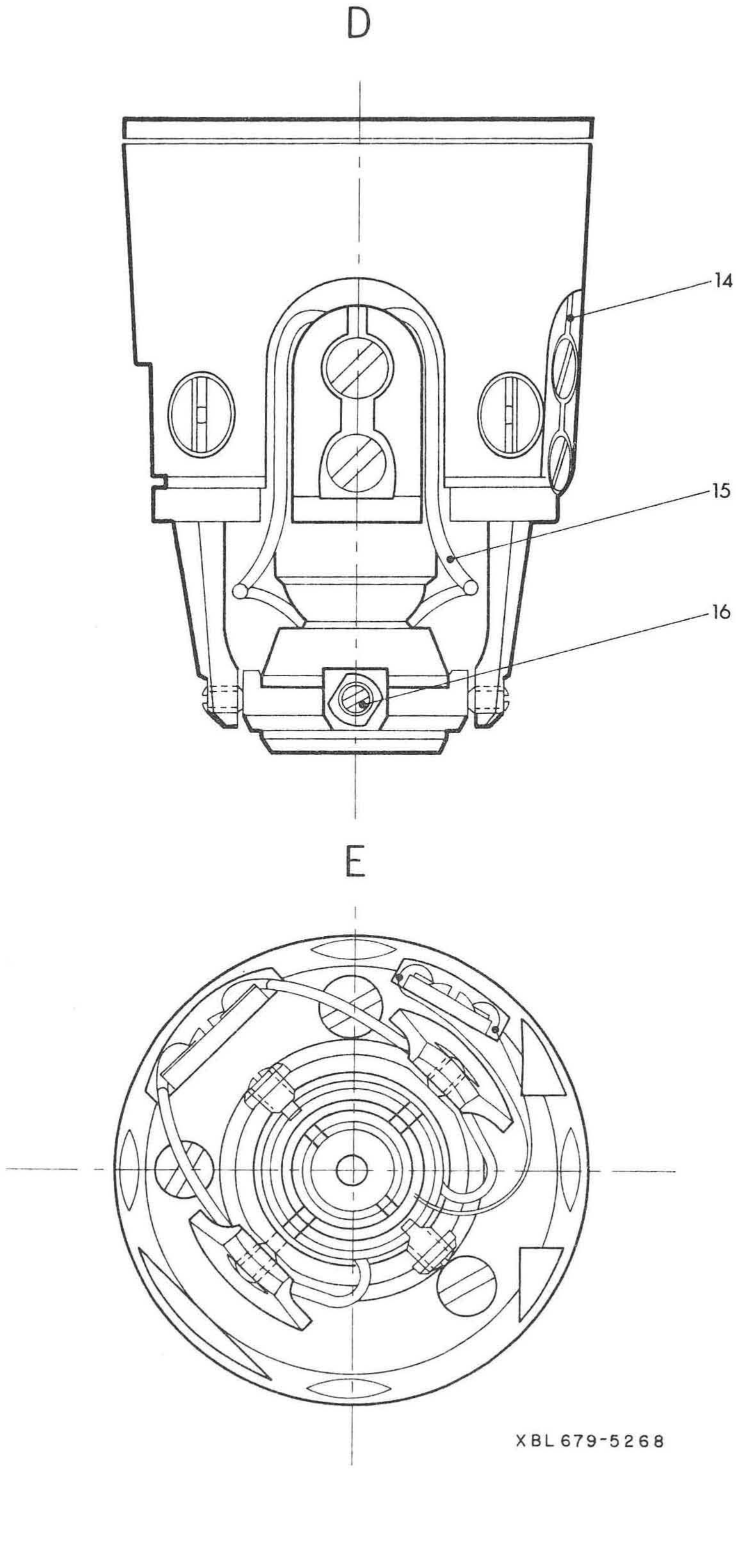

Figure 2.

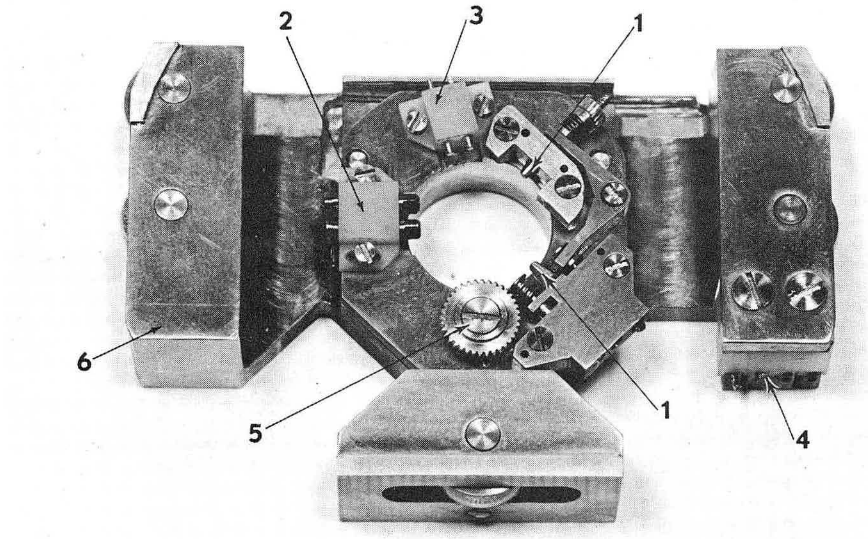

XBB 679-5508

Fig. 3 Modified Object Stage.

1. Pusher pins for tilting.
2. Spring loaded contact pins. These pins contact the heater circuit board when the specimen holder is inserted.
3. Spring loaded contact pins. These pins contact the thermocouple circuit board when the specimen holder is inserted.
4. Electrical connecting posts for heater and thermocouple connecting wires (see also Fig. 9c).
5. Worm and gear to drive a rotating-tilting specimen holder (see Valdre, ref. 3).
6. Object stage.

All parts are bronze except the Delrin mounts for the contact pins. The copper contact pins (2) and the Pt and Pt-10%Rh contact pins (3).

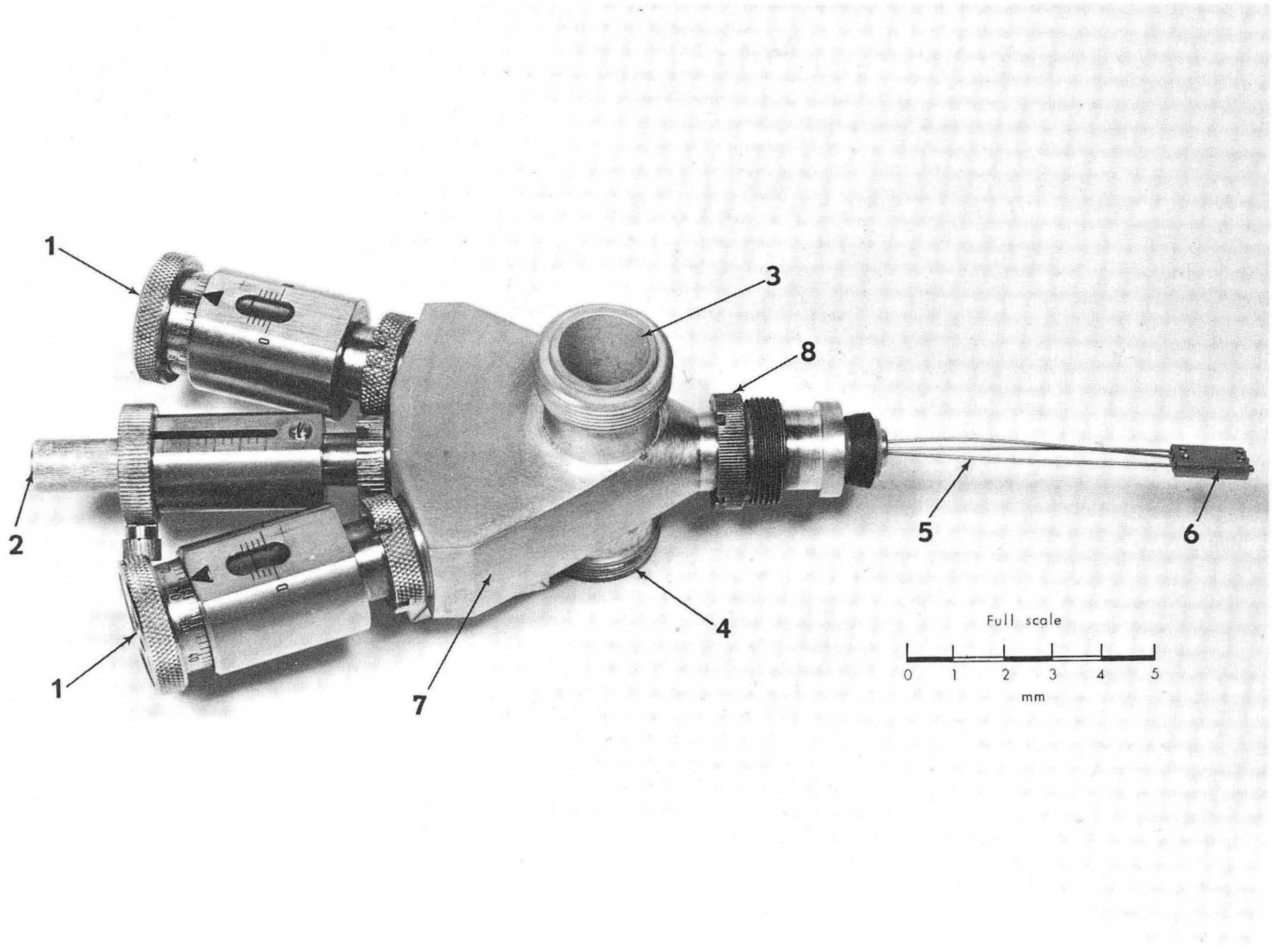

XBB 679-5509-A

Fig. 4 Triple Drive System.

1. Tilt drives.
2. Rotation drive (see ref. 3).
3. Auxilliary port.
4. Electrical leads port. (Ports 3 and 4 are vacuum sealed with "O" rings.)
5. Drive wires for tilting.
6. Positioners for engaging wires in object stage.
7. Main body of triple drive system.
8. Nut for screwing drive in stero hole of microscope.

The Siemens stero driver (1), the drive connecting nut (8) and the drive wires (5) are stainless steel. The rest of the parts are bronze.

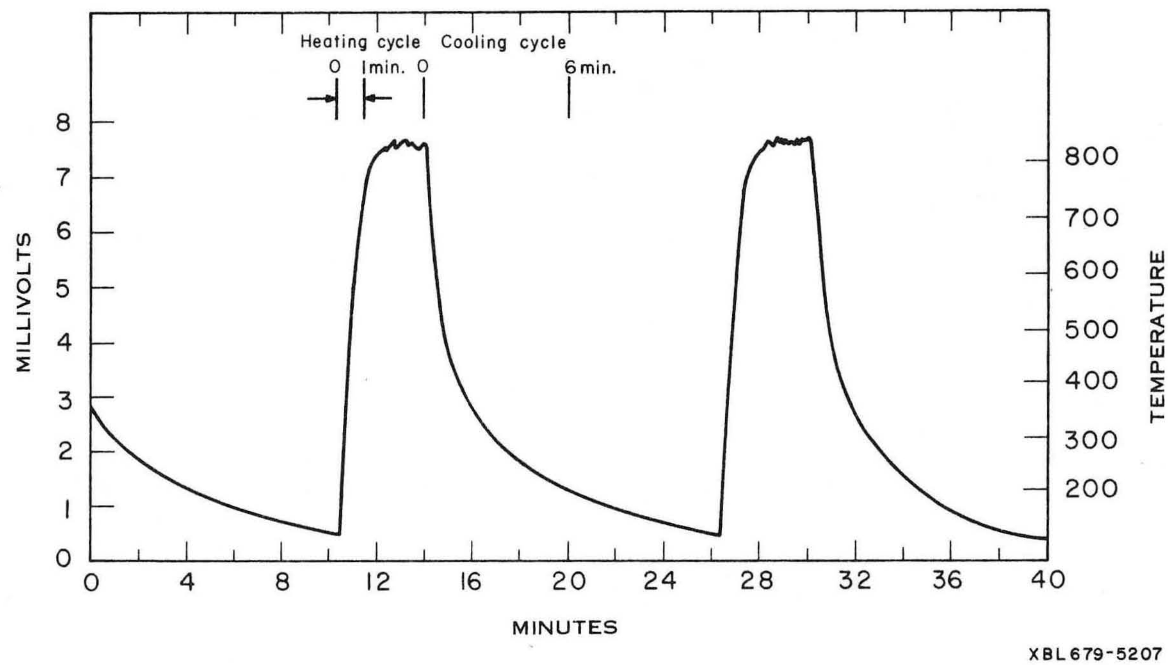

Fig. 5 Time-Temperature Response Cycles of the Heating and Tilting Specimen Holder.

Two complete heating and cooling cycles are shown. The power is turned on to maximum value at time zero (points A) then turned off completely when the thermocouple voltage has leveled off at its maximum value for the power being used (points B). The holder reaches a temperature of 825°C in about one minute. It cools from 825° to 200°C in six minutes.

Fig. 6 Hexagonal to Face Centered Cubic Transformation of Cobalt.

Figures 6a and 6b show the microstructure and selected area diffraction (SAD) pattern of 80% cold rolled cobalt sheet at room temperature. The diffraction rings d_1, d_2, d_3 and d_4 are respectively the $[10\bar{1}0]$, $[10\bar{1}1]$, $[11\bar{2}0]$ and $[10\bar{1}2]$ planes of the close packed hexagonal structure. Figures 6c and 6d show the microstructure and SAD pattern of the same area after the foil is heated to 450°C. The SAD pattern shows spots from many FCC grains and ring structure from either small FCC grains or residual HCP as rolled grains.

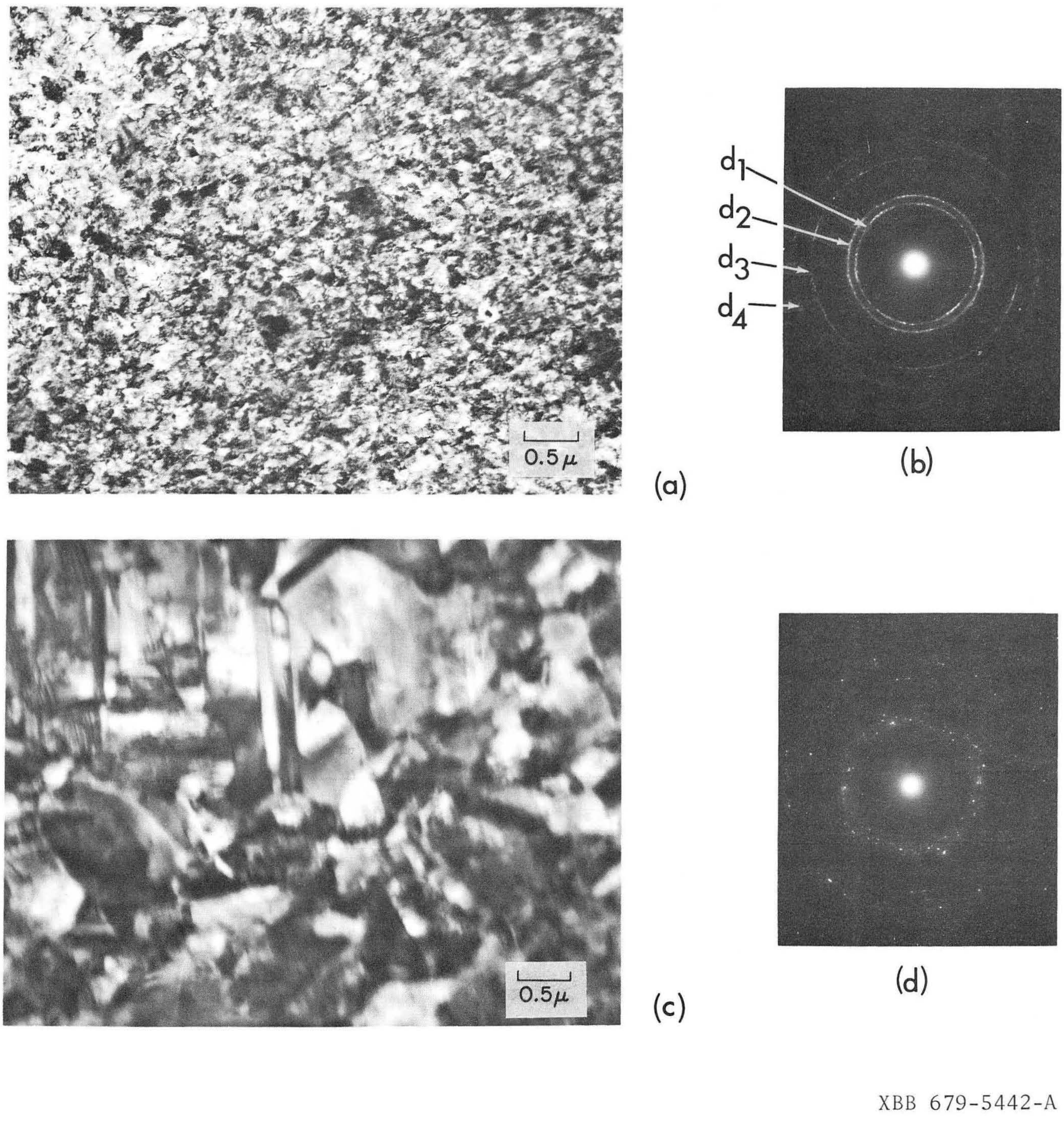

XBB 679-5442-A

Fig. 6

Fig. 7. Temperature Sensitivity of Magnetic Domain Walls.

The domain walls are about 200 Å thick and are imaged by the out-of-focus method.[6] The foil orientation (Fig. 7b) was maintained for all three micrographs. The foil orientation is normal to $[\bar{1}2\bar{1}0]$ and the reciprocal lattice vectors shown are $\bar{g}_1 = [20\bar{2}1]$ and $\bar{g}_2 = [0002]$. Note that $\bar{g}_2$ is parallel to the domain walls. As the temperature is heated to 150°C (Fig. 7c) the domain walls, A, widen and become diffuse and difficult to focus. Finally at 300°C (Fig. 7d) no domain structure is visible.

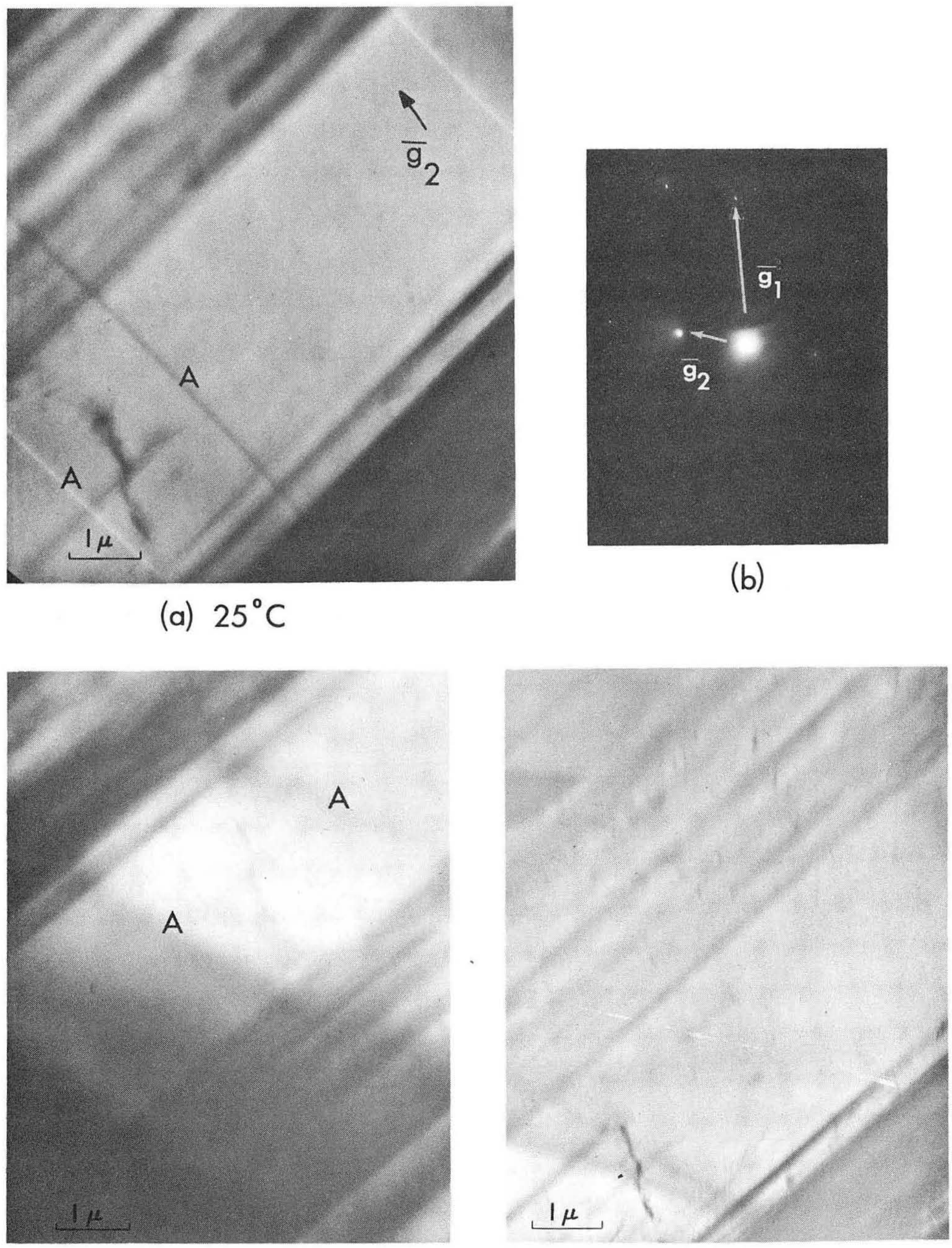

(a) 25°C (b)

(c) 150°C (d) 300°C

XBB 679-5443-A

Fig. 7

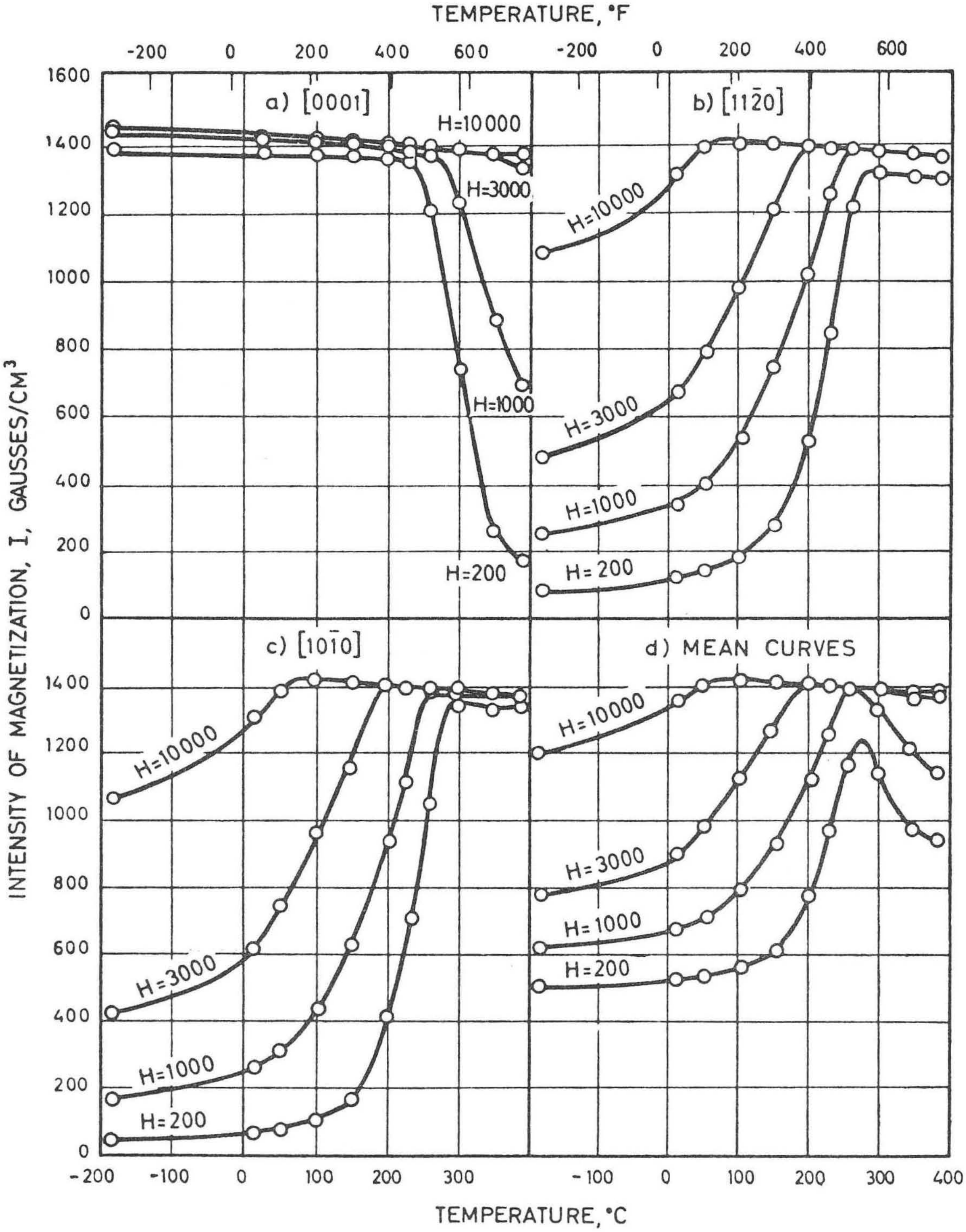

FIG. 8 EFFECT OF TEMPERATURE ON THE MAGNETIZATION OF HEXAGONAL COBALT
(After Honda and Masumoto[10])

XBL 683-2206

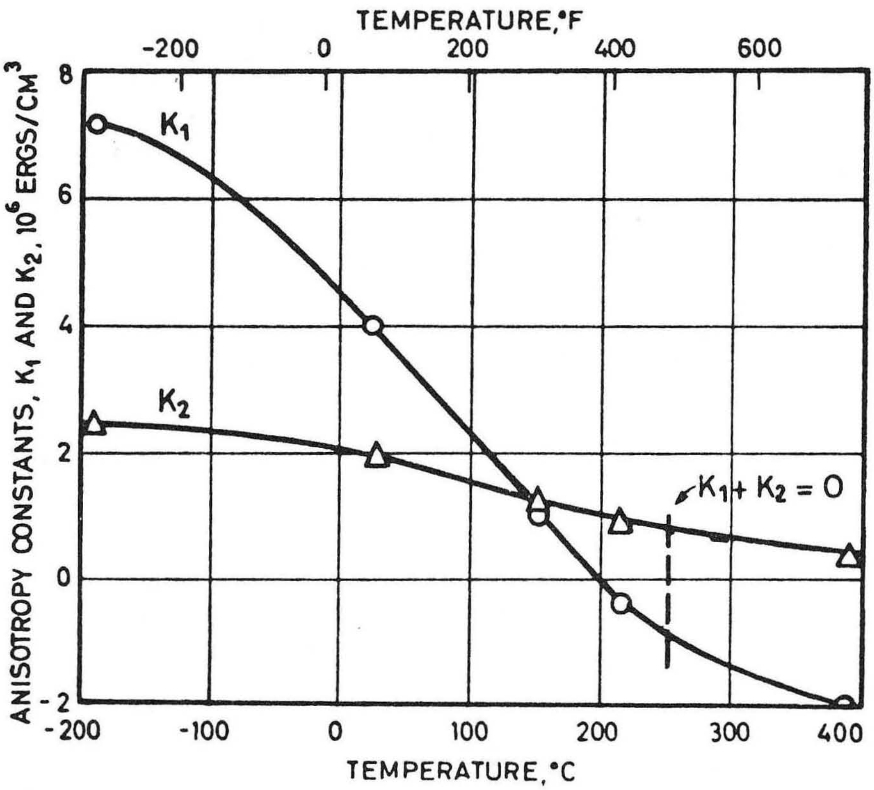

FIG. 9 CRYSTAL ANISOTROPY CONSTANTS OF COBALT AT VARIOUS TEMPERATURES
(After Honda and Masumoto[10])

XBL 683-2207

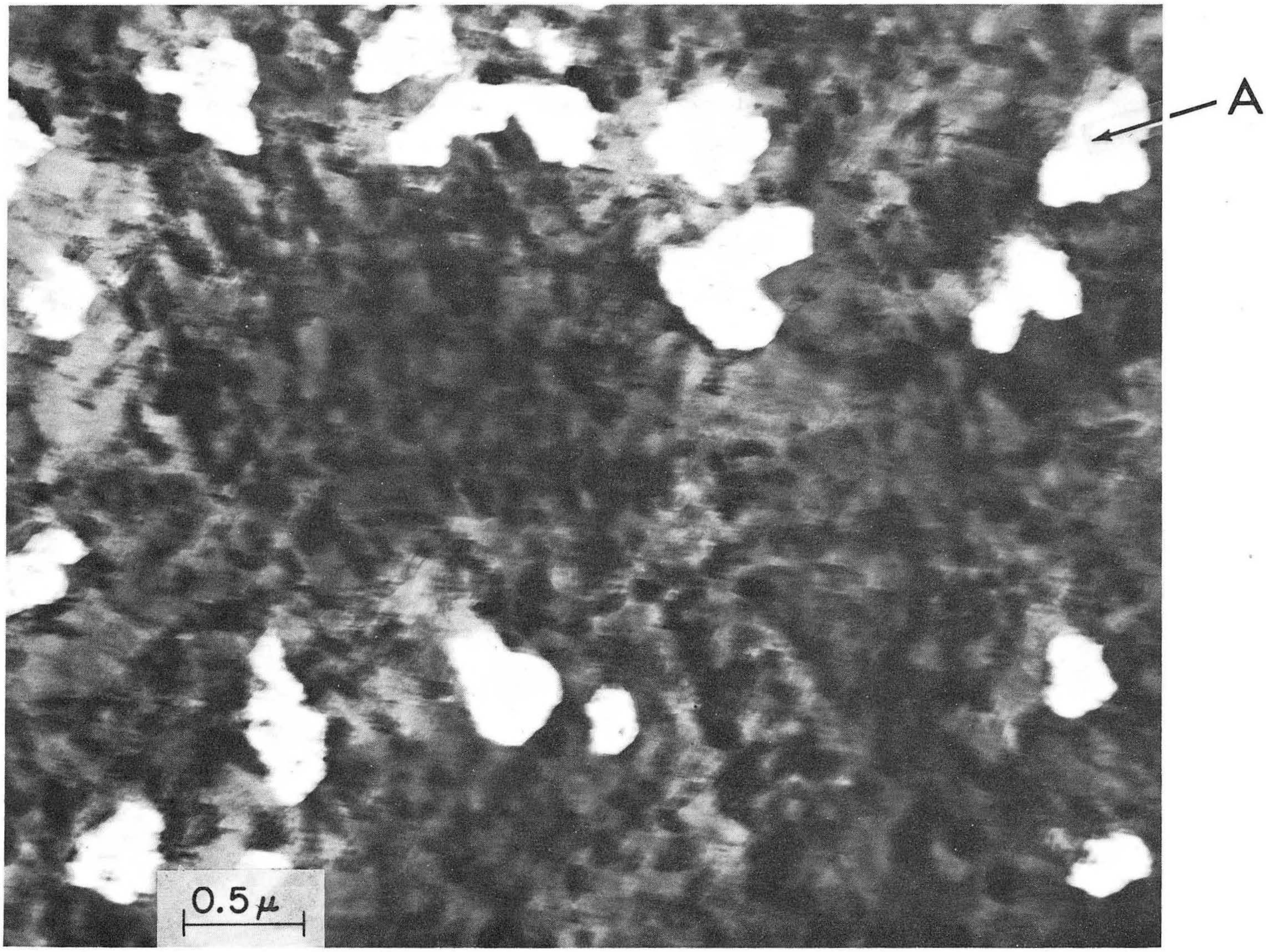

XBB 679-5444-A

Fig. 10.

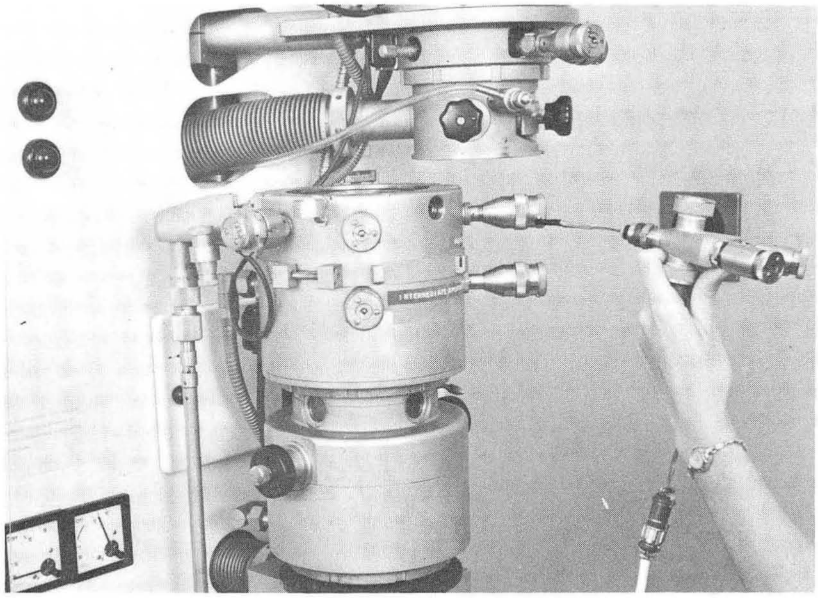

(a)

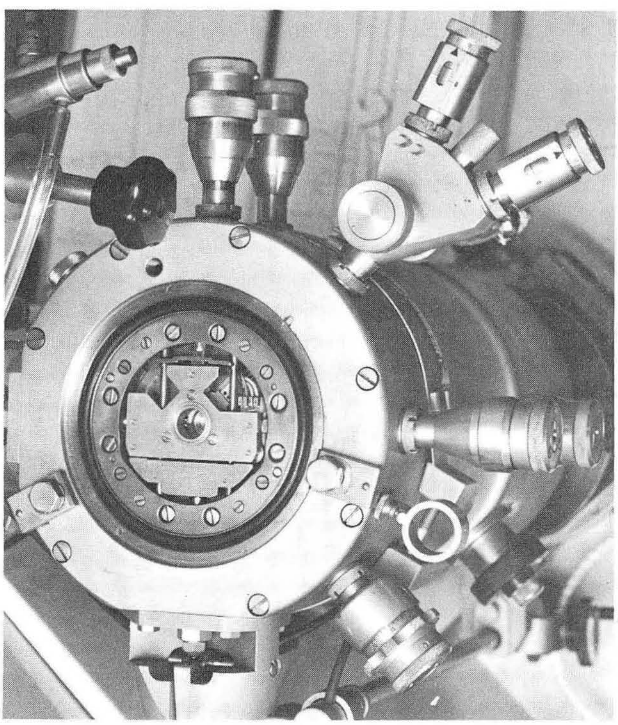

(b)

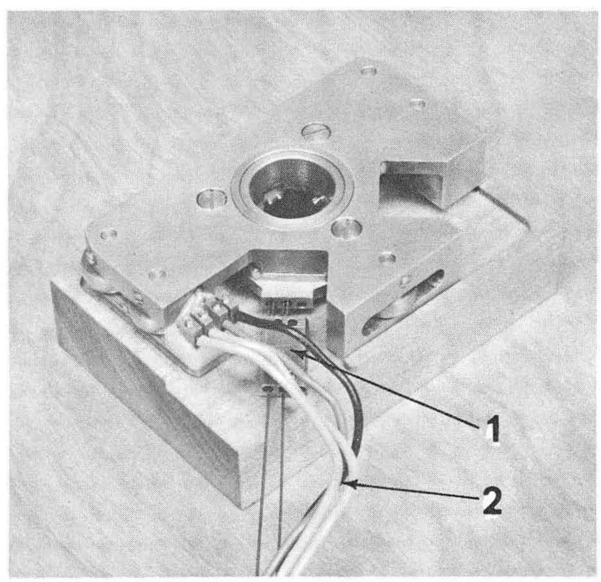

(c)

XBB 679-5445

Fig. 11

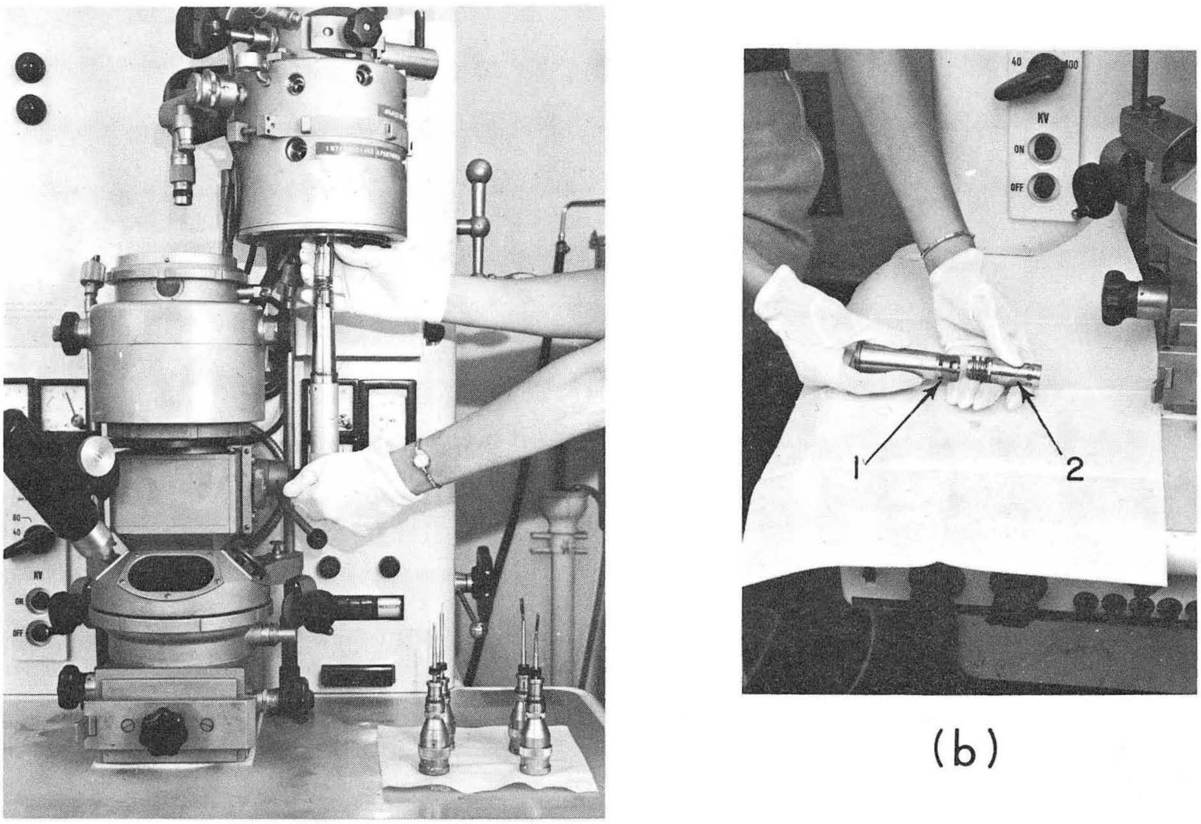

(a) (b)

XBB 679-5446-A

Fig. 12

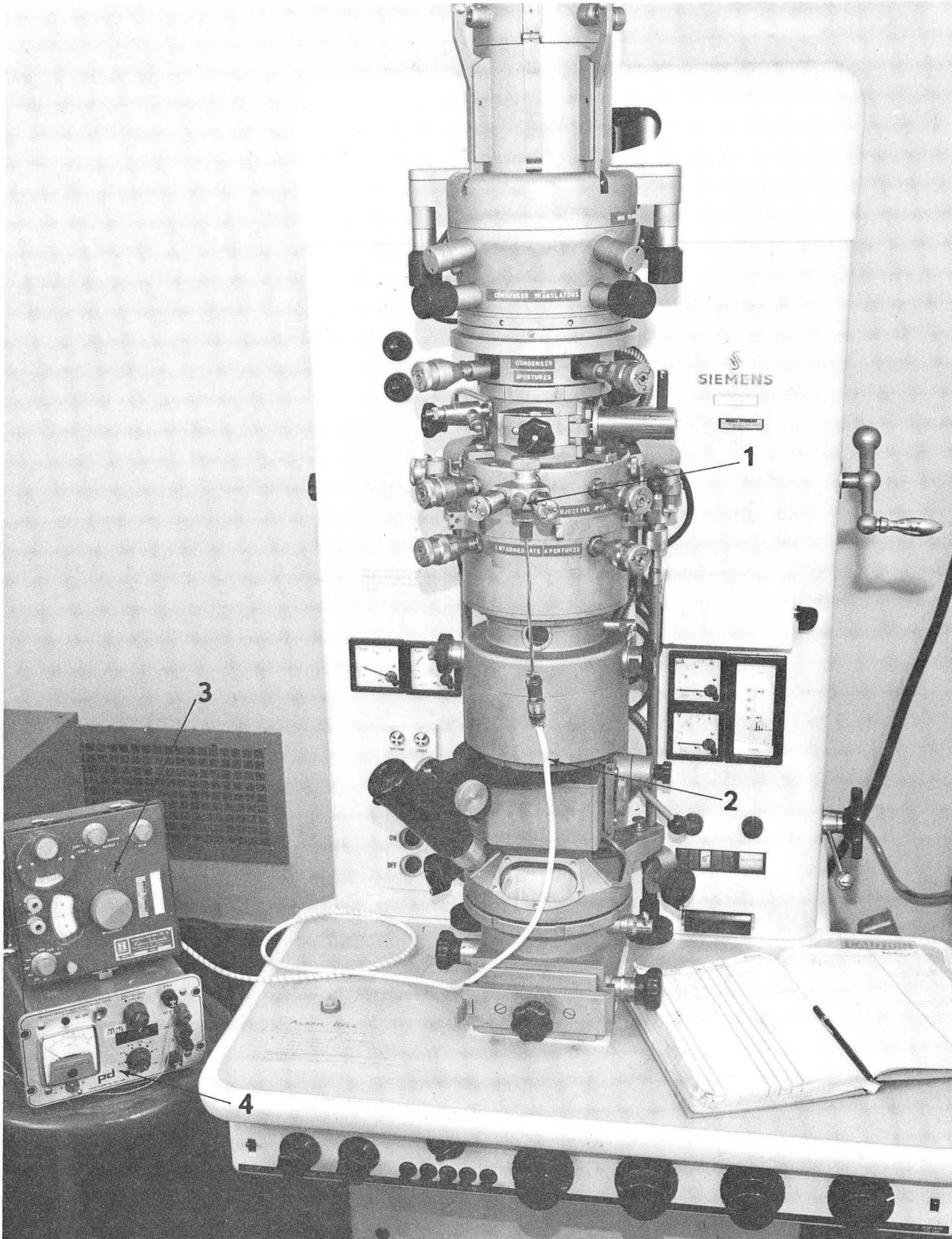

Fig. 13 XBB 679-5510